



# January 24, 2020 Sivrice-Elazığ (Türkiye) Earthquake: The Seismic Assessment of the Earthquake Territory, Geotechnical Findings and Performance of Masonry Buildings

İbrahim Özgür Dedeoğlu<sup>1</sup> · Musa Yetkin<sup>2</sup> · Yusuf Calayır<sup>2</sup> · Hakan Erkek<sup>3</sup>

Received: 27 June 2023 / Accepted: 25 November 2023 / Published online: 18 December 2023  
© The Author(s), under exclusive licence to Shiraz University 2023

## Abstract

On January 24, 2020, an 6.8 magnitude ( $M_w$ ) earthquake struck the Sivrice district of Elazığ province in south-eastern Türkiye. The earthquake, which occurred in the East Anatolian Fault Zone (EAFZ), affected many structures. In particular, most of the masonry buildings close to the epicenter were severely damaged or destroyed and the earthquake resulted in 41 fatalities. This paper aims to provide information on the tectonic characteristics of the EAFZ, the seismic characteristics of the earthquake territory and the general characteristics of the main shock. Another purpose of this paper is to reveal the damage caused by the earthquake to the masonry buildings in rural areas through post-earthquake field observations. As a result of the field observations, the types of damage seen in masonry structures are poor workmanship and binder damages, in/out of the plane mechanism, damages due to the absence of lintels or insufficient lintel length, weak load-bearing walls damage, corner damages and multi-leaf walls damages. The most important reason for the damage to the structures is the lack of engineering services and not being constructed in accordance with earthquake codes. In addition, considering the damage to the masonry buildings as a result of the field studies, some retrofitting methods are presented for strengthening existing masonry buildings with low seismic performance against future earthquakes.

**Keywords** January 24 2020 Sivrice-Elazığ earthquake · East anatolian fault zone · Masonry buildings · Field investigation · Earthquake performance

## 1 Seismicity of the Territory

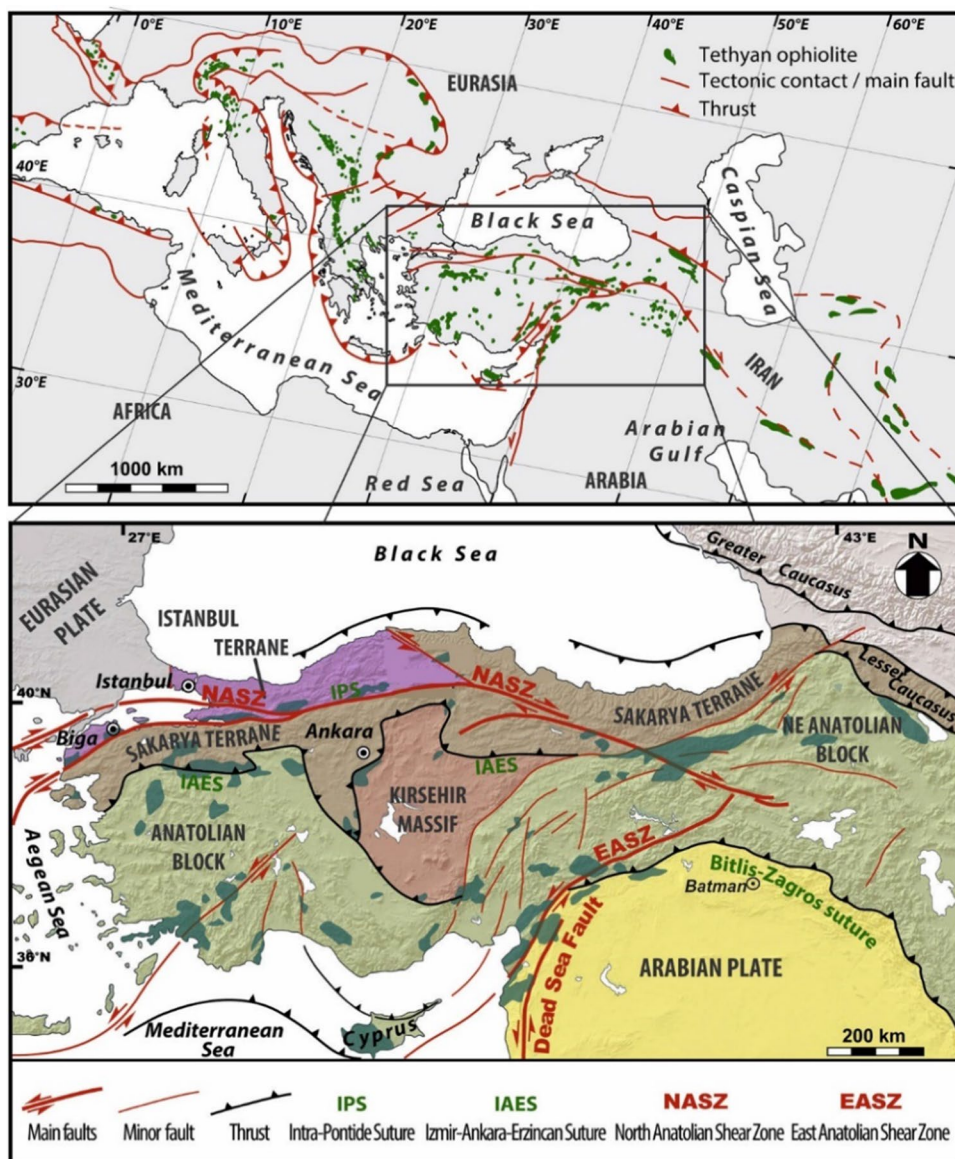
Türkiye is located on the borders of the Eurasian, African and Arabian plates and has active tectonic structures, such as the North Anatolian Fault Zone (NAFZ), East Anatolian Fault Zone (EAFZ), Bitlis Zagros Suture Belt (BZSB) (Fig. 1). Among these fault zones, the North Anatolian Fault Zone has a right-lateral strike-slip mechanism, and the East Anatolian Fault Zone has a left-lateral strike-slip mechanism (Bozkurt 2001).

EAFZ is composed of six main segments, namely Karlıova-Bingöl, Palu-Hazar, Hazar-Sincik, Çelikhanköy, Gölbaşı-Türkoğlu and Türkoğlu-Antakya. The lengths of these fault segments range between 31 and 112 km (Okay et al. 2010). The January 24, 2020 Sivrice-Elazığ earthquake occurred on the Hazar-Sincik fault segment of EAFZ. The length of this fault is around 80 km and surface deformation has been observed along 48 km of the total length (Kürçer et al. 2020). In addition, a calculated rupture of 40 km was reported by the Disaster Emergency and Management

✉ Musa Yetkin  
musayetkin@firat.edu.tr  
İbrahim Özgür Dedeoğlu  
iozgur.dedeoglu@batman.edu.tr  
Yusuf Calayır  
ycalayir@firat.edu.tr  
Hakan Erkek  
hakanerkek@gmail.com

<sup>1</sup> Department of Civil Engineering, Batman University, Batman, Turkey  
<sup>2</sup> Department of Civil Engineering, Fırat University, Elazığ, Turkey  
<sup>3</sup> Department of Civil Engineering, Osmaniye Korkut Ata University, Osmaniye, Turkey

**Fig. 1** NAFZ, EAFZ, BZSB, and other important tectonic structures in the Geology of Türkiye (Adopted from Mar-roni et al. 2020)



Authority (DEMA) for the January 24, 2020 Sivrice-Elazığ earthquake (DEMA 2020a). However, more research is needed to know how much of this fault was ruptured during the main shock. Historical disastrous earthquakes on the EAFZ were demonstrated in Fig. 2 along with the January 24, 2020 Sivrice-Elazığ earthquake.

Elazığ city is a region with quietly high seismicity, most of which is located on the EAFZ. The eastern part of the EAFZ starting from Palu-Hazar continues to the southwest with the Hazar-Sincik segment. This segment determines the seismicity of the region. The country is divided into five zones in the Seismic Zoning Map published by the Türkiye Ministry of Public Works and Settlement in 1996 (Fig. 3). The majority of Elazığ city is in the first-degree earthquake zone (design acceleration is  $A_0=0.4$  g), while the other regions are in the second-degree zone ( $A_0=0.3$  g).

On January 1, 2019, the new “Türkiye Earthquake Hazard Map” was published with a considerably renewed (Fig. 4). This new map shows peak map acceleration values (PGA) instead of earthquake zones. The maximum acceleration value for the design earthquake (an earthquake with a return period of 475 years and earthquake % 10 probability of exceedance in 50 years) for the Elazığ region of the Hazar-Sincik segment varies between 0.6 and 0.7 g. This situation shows that the earthquake risk of the region is relatively high, especially within the Eastern Anatolian Fault Zone.

Many researchers have studied damages caused by earthquakes in the past. The earthquake performance of the reinforced concrete (RC) structures is evaluated by Sezen et al. (2003) for the 1999 Kocaeli earthquake and by Doğançün (2004) for the 2003 Bingöl earthquake. Hosseini (2005) presented the damages and behavior of

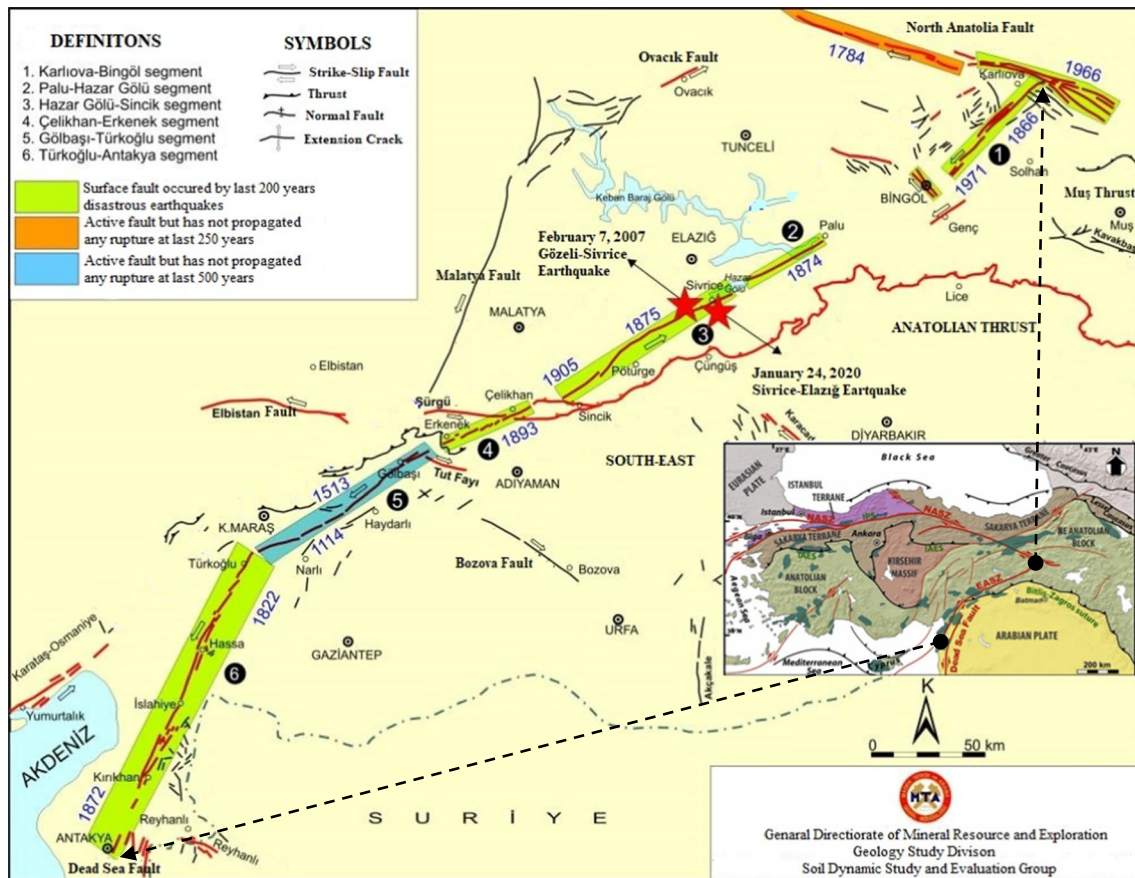
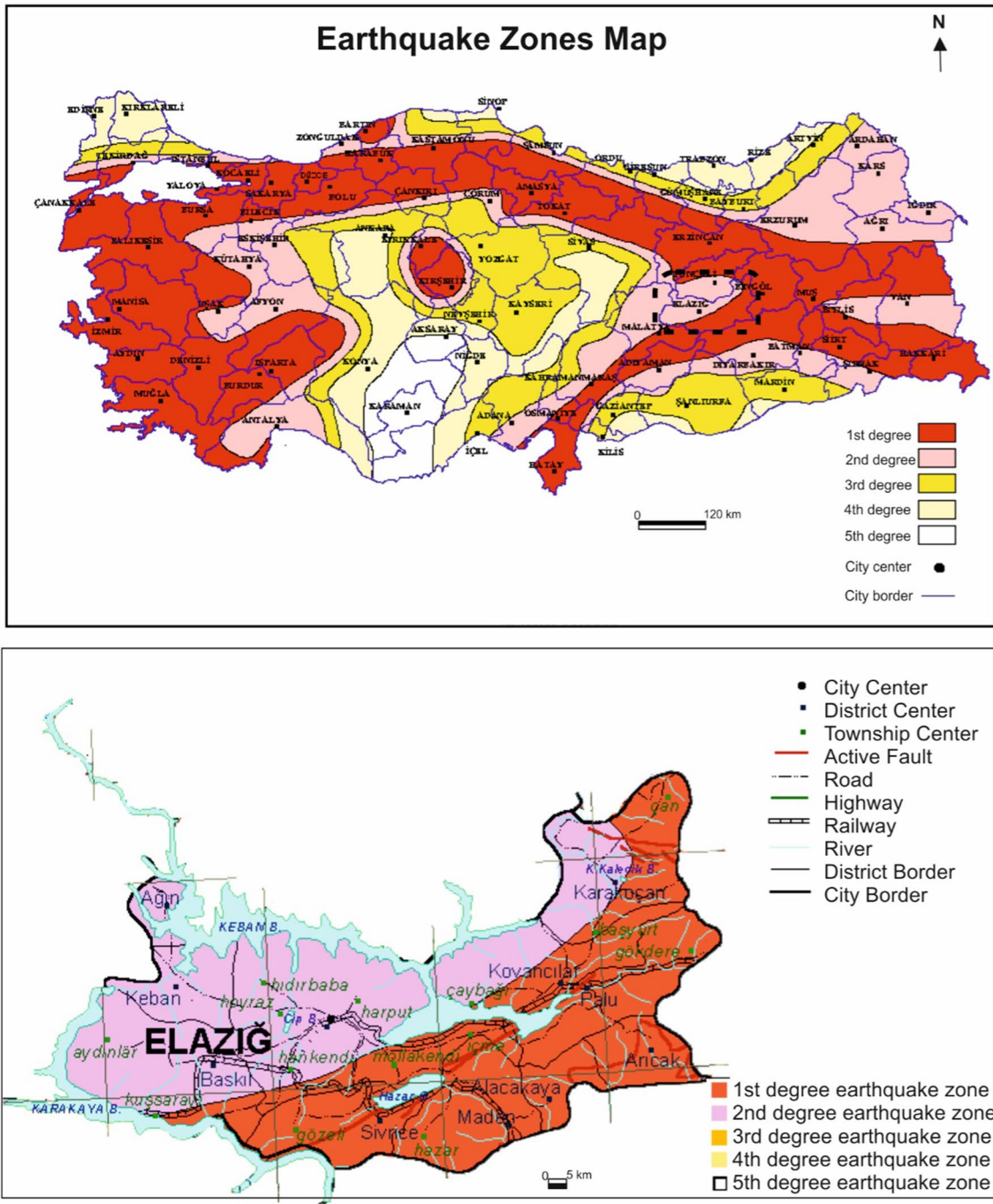


Fig. 2 Main segments of the EAFZ and Historical Disastrous Earthquakes (Adopted from Şaroğlu et al. 1992)

non-structural elements in the 2003 Bam, Iran, Earthquake. Rossetto and Peiris (2009) presented observations of damage due to the Kashmir earthquake (2005) and study of current seismic provisions for structures in Pakistan used for the reconstruction of affected areas. Celep et al. (2011) investigated failures of masonry and RC structures during the March 8, 2010 Kovancılar and Palu Earthquakes in Elazığ, Türkiye. Calayır et al. (2012) assessed damages of various structures (adobe, masonry, hımış, and RC structures, and minarets) in the rural area during the March 8, 2010 Kovancılar Earthquakes in Elazığ, Türkiye. Ricci et al. (2011) presented an analysis of the main damage that RC structures shown after 2009 L'Aquila earthquake. Bayraktar et al. (2013), Bayraktar et al. (2014), Sayın et al. (2014) and Bayraktar et al. (2015) investigated construction failures in masonry buildings after the 2011 Van Earthquake and emphasized that the main reasons for the damage were poor workmanship, use of low-quality structural materials, superficial detailing of construction elements and lack of engineering services. Sharma et al. (2016) investigated the effects on masonry and reinforced concrete buildings after the 2015 Gorkha earthquake in Nepal. Brando et al. (2017) investigated the damage after

the 2009 L'Aquila earthquake and developed a predictive model for masonry buildings. Sisti et al. (2019) produced a damage assessment of masonry buildings after the 2016 Central Italy earthquake. Basaglia et al. (2020) investigated post-earthquake damage for both masonry and reinforced concrete buildings in a town affected by the 2012 Northern Italy earthquake. Sayın et al. (2021) presented a comprehensive study on January 24, 2020 Sivrice-Elazığ, Türkiye. Günaydın et al. (2021) examined the case studies of damaged masonry buildings and failure or collapse mechanisms. Yetkin et al. (2021) investigated the damages that occurred at the minarets in Elazığ after the January 24, 2020 Sivrice-Elazığ earthquake. At the end of the study, some recommendations were made for the repair and strengthening of damaged minarets and the construction of new minarets. Dedeoğlu et al. (2022) examined the damages caused by the earthquake in the RC buildings in Elazığ, with the post-earthquake field observations. The main causes of the damage have been presented and discussed in detail.

On January 24, 2020, an  $M_w = 6.8$  (DEMA 2020b) earthquake occurred in the Sivrice district of the city of



**Fig. 3** Seismic zoning maps of Türkiye and Elazığ city (The 1996 earthquake zonation map (<https://www.afad.gov.tr/turkiye-deprem-tehlike-haritasi>) Zone 1 (red) represents the highest seismic hazard

whereas pink, yellow and light yellow colors represent Zones 2, 3 and 4 that display the decreasing trend in seismic hazard. The white color is the no seismic hazard zone)

Elazığ. The event caused casualties and severe damage to buildings, lifelines and other infrastructures. The authors carried out a field survey in the city center, in the districts, and in the villages of Elazığ to assess the extent of

the damage to the masonry buildings. The purpose of this paper is to examine and discuss the damage and collapse mechanisms observed in Elazığ city’s masonry buildings during the earthquake, to summarize the past and present

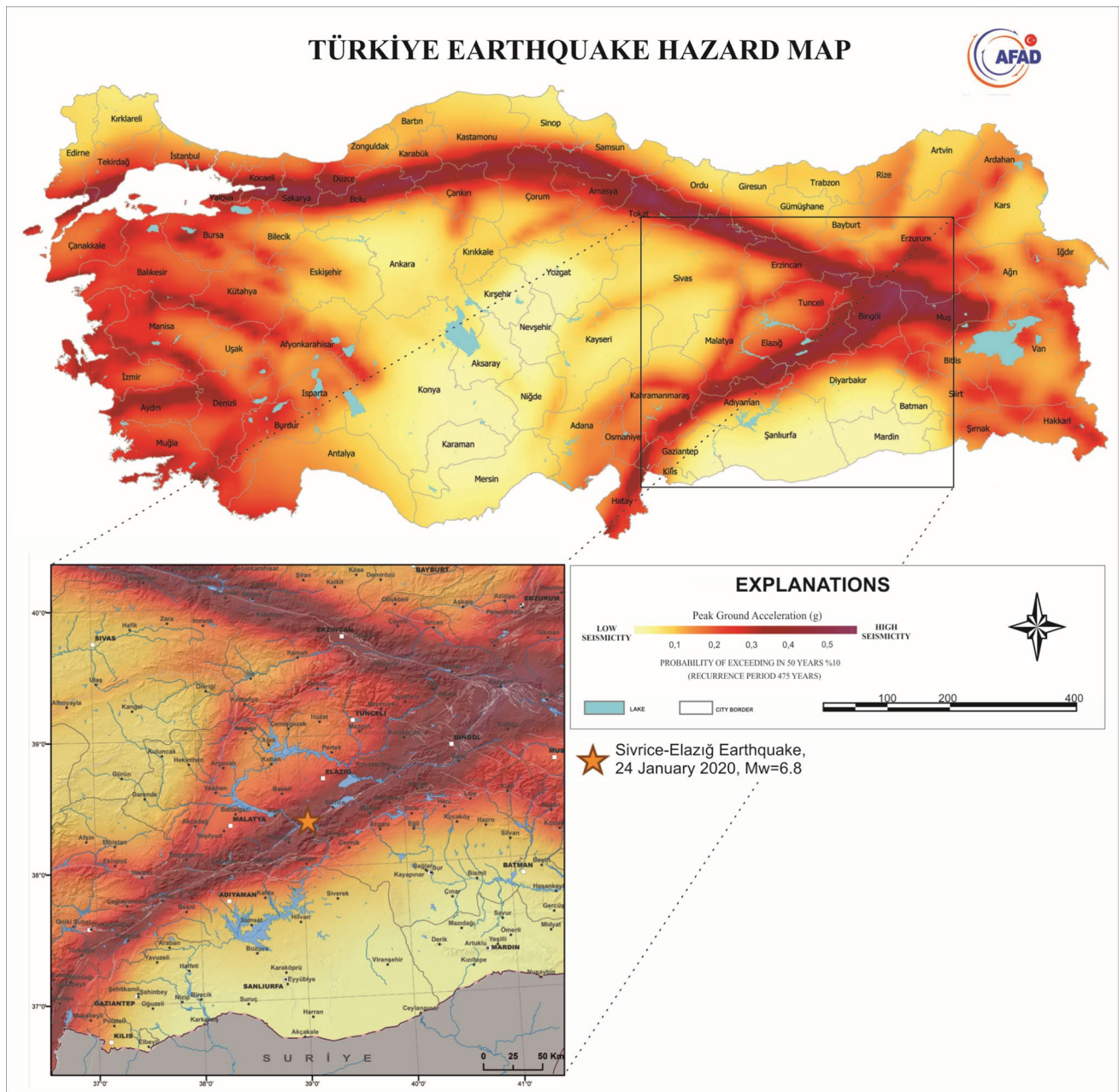


Fig. 4 Türkiye Earthquake Hazards Map and seismicity of the region of earthquake occurred (Adopted from DEMA 2020b)

seismotectonic characteristics of the EAFZ, present the seismological characteristics and recorded accelerograms

of the earthquake, followed by our conclusions and recommendations based on the field observations.

**Table 1** Earthquake parameters obtained from various institutions (DEMA 2020a)

Parameter	DEMA	KOERI	INGV	GFZ	USGS	CSEM
Location	38.36 N 39.06 E	38.37 N 39.24 E	38.39 N 39.12 E	38.36 N 39.20 E	38.39 N 39.08 E	38.37 N 39.22 E
M <sub>w</sub>	6.8	6.5	6.8	6.8	6.8	6.7
Depth (km)	8.06	5.0	11.0	10.0	11.9	15.0

**Table 2** Ground motion characteristics of the January 24, 2020 Sivrice-Elazığ earthquake, as recorded by some accelerometer stations (DEMA 2020a)

Station					Measured acceleration values (g)			Distance (km)			
Code	Province	District	N	E	N-S	E-W	U-D	$R_{jb}$	$R_{rup}$	$R_{epi}$	$R_{hyp}$
2308	Elazığ	Sivrice	38.45	39.91	0.2405	0.2985	0.1821	17.86	17.89	23.81	25.14
4404	Malatya	Pütürge	38.20	38.87	0.2117	0.2438	0.1495	18.60	18.63	24.55	25.84
2301	Elazığ	City Center	38.67	39.19	0.1205	0.1405	0.0672	30.43	30.46	36.39	37.27
0204	Adıyaman	Gerger	38.03	39.03	0.0962	0.1123	0.0604	30.86	30.88	36.81	37.69
0212	Adıyaman	Sincik	38.03	38.62	0.0444	0.0393	0.0325	47.25	47.26	53.21	53.81
2302	Elazığ	Maden	38.39	39.68	0.0261	0.0320	0.0232	47.56	47.57	53.51	54.11
2104	Diyarbakır	Ergani	38.26	39.76	0.0273	0.0261	0.0246	55.68	55.69	61.64	62.16
4401	Malatya	Battalgazi	38.35	38.34	0.0747	0.0894	0.0381	57.08	57.09	63.04	63.55
0205	Adıyaman	Kâhta	37.79	38.62	0.0260	0.0418	0.0265	68.30	68.31	74.25	74.69
0207	Adıyaman	Çelikhan	38.03	38.25	0.0322	0.0299	0.0179	74.04	74.05	80.00	80.40

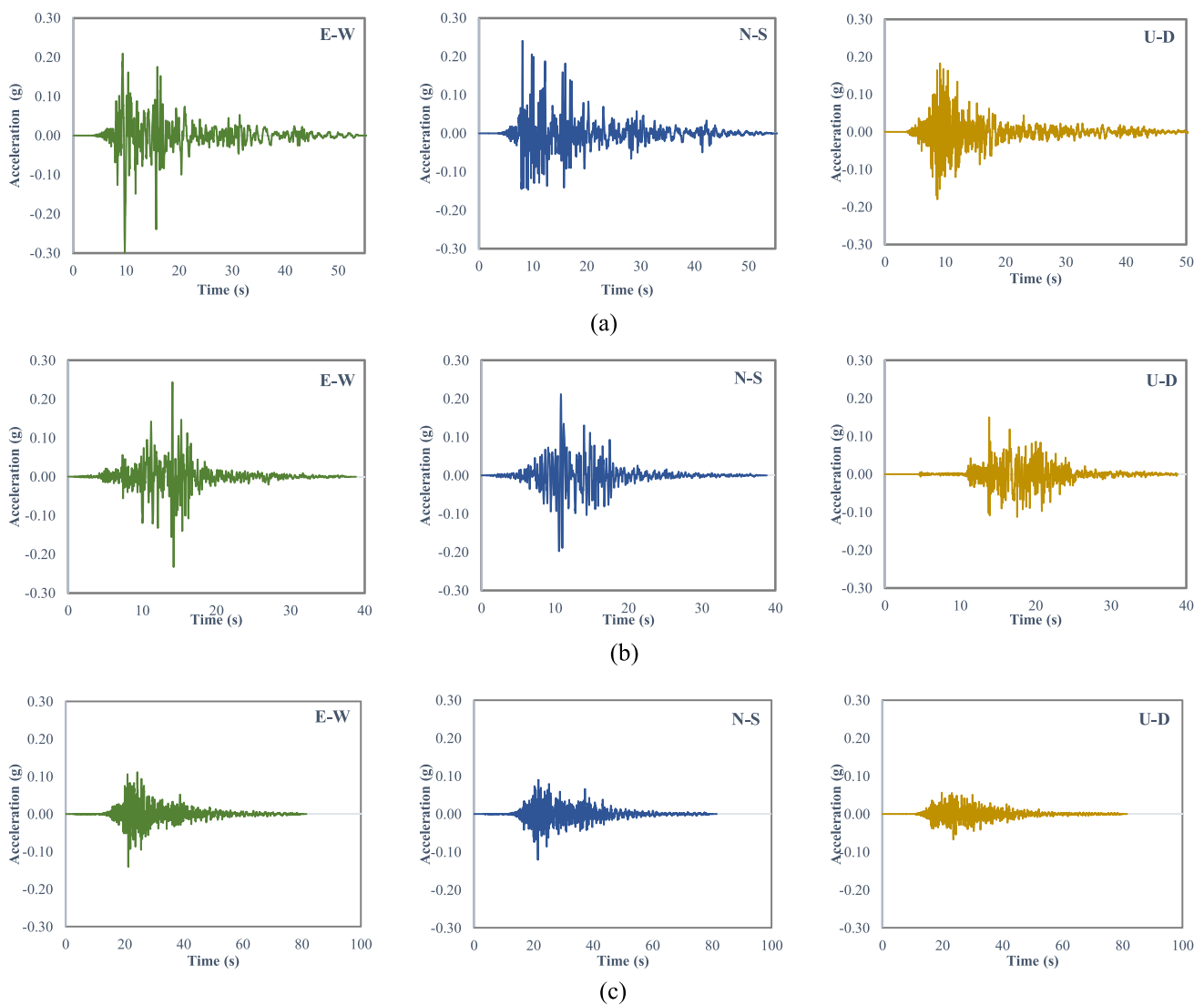


**Fig. 5** Three components of ground accelerations of the January 24, 2020 Sivrice-Elazığ earthquake, as recorded at **a** Sivrice, **b** Pütürge and **c** Elazığ-City Center stations

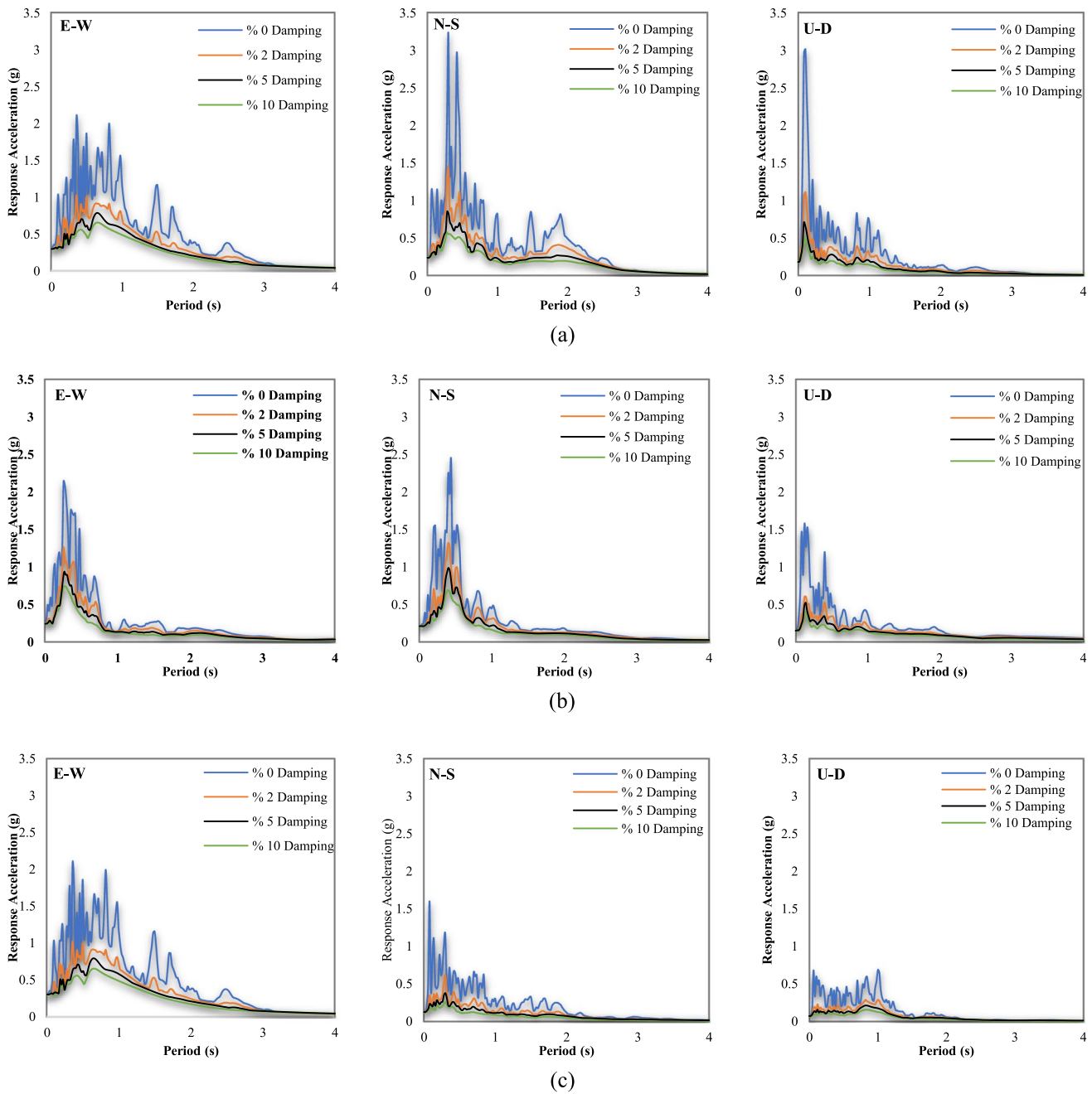


**Fig. 6** The acceleration response spectra of **a** the Sivrice station record, **b** the Pütürge station record and **c** the Elazığ-City Center station record for the damping ratio of 0%, 2%, 5% and 10% of the E-W, N-S and U-D components

## 2 Seismic Characteristics of the Earthquake

The January 24, 2020 Sivrice-Elazığ earthquake is the largest earthquake to occur on the EAF in the twenty-first century. This strong ground motion was announced by DEMA as  $M_w = 6.8$ . The magnitude of the earthquake was also recorded by different national and international seismological stations. The earthquake parameters taken from various institutions are given in Table 1. The reported

magnitude and depth ranged between 6.5 and 6.8 ( $M_w$ ) and 5.0–15.0 km, respectively.

Table 2 presents some detailed ground motion characteristics of the January 24, 2020 Sivrice-Elazığ earthquake, peak ground acceleration values and distance to the earthquake source for various distance units ( $R_{epi}$ ,  $R_{rup}$ ,  $R_{JB}$ ,  $R_{hyp}$ ). Here,  $R_{epi}$  is the earthquake's epicenter distance,  $R_{rup}$  is the rupture distance,  $R_{JB}$  is Joyner-Boore distance and  $R_{hyp}$  is the focal distance. As can be seen, the closest station is

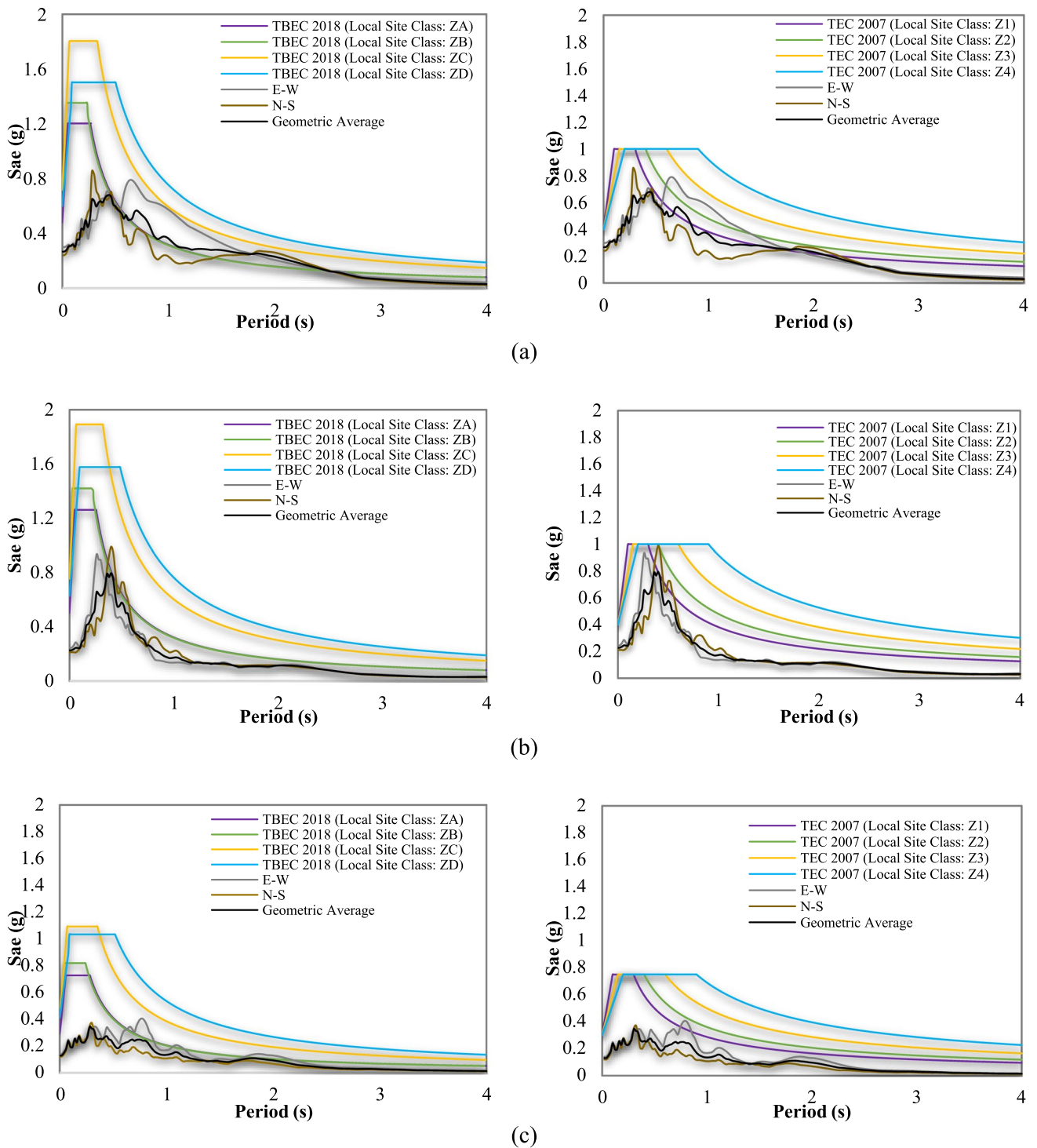


**Fig. 7** Comparisons of acceleration response spectra with design spectra TEC (2007) and TBEC (2018) for **a** the Sivrice station record, **b** the Pütürge station record and **c** the Elazığ-City Center station record

Sivrice (2308), which is located on the fault at a distance of 23.81 km from to epicenter. In addition, the peak ground acceleration was recorded as 0.2985 g.

The peak ground acceleration values were obtained at the Sivrice (2308), Pütürge (4404) and Elazığ-Center (2301)

stations. The three ground acceleration component records of the earthquake obtained from these stations are given in Fig. 5. The peak ground accelerations were obtained at the Sivrice station with values of 0.2985 m/s<sup>2</sup> for the E–W component, 0.2405 m/s<sup>2</sup> for the N–S component and 0.1821 m/





**Fig. 8** Small-scale mass movements and stone falls due to these movements

$s^2$  for the U-D component. The peak ground accelerations were obtained at the Malatya-Pütürge station with values of  $0.2438 \text{ m/s}^2$  for the E-W component,  $0.2117 \text{ m/s}^2$  for the N-S component and  $0.1495 \text{ m/s}^2$  for the U-D component. The peak ground accelerations for E-W, N-S and U-D components were measured as  $0.1405 \text{ m/s}^2$ ,  $0.1205 \text{ m/s}^2$  and  $0.0672 \text{ m/s}^2$ , respectively, at the Elazığ-Center station. It should be noted that the peak ground accelerations recorded at the Sivrice and Pütürge stations did not exceed the peak ground acceleration set by Türkiye Earthquake Code (TEC 2007) (0.3–0.4 g) and Türkiye Building Earthquake Code (TBEC 2018) (0.6–0.7 g) earthquake hazard maps. In addition to Elazığ-Center stations did not exceed the peak ground acceleration set by both earthquake hazard maps.

Figure 6 shows the acceleration response spectra calculated for both the Sivrice, Pütürge and Elazığ-City center station records, for damping ratios of 0%, 2%, 5% and 10% for the E-W, N-S and U-D components.

In Fig. 7, the acceleration response spectra of the E-W, N-S and U-P components with 5% damping were compared with the design spectra specified in the TEC (2007) for the local site class Z1, Z2, Z3 and Z4, and TBEC (2018) for the local site classes ZA, ZB, ZC, and ZD. These were calculated for the locations in the Sivrice, Pütürge and Elazığ city center districts where the peak ground acceleration occurred. The earthquake design hazard level was determined for earthquake ground motion, with 10% probability of exceedance within 50 years. As can be seen in Fig. 7, The spectra of the earthquake acceleration records were generally below the design spectra. Also, TBEC (2018) allows safer design.

### 3 Geotechnical Finding

Considering the geotechnical effects of the earthquake, small-scale mass movements were observed in the north of Hazar Lake and the northern cuts of the highway between Elazığ and Sivrice and large stone falls on the highway due to these movements (Fig. 8). In addition, cracks formed on the asphalt highway connecting the Çevrimtaş village where the earthquake occurred and parallel to the road route were determined. It was observed that the width of these cracks exceeded 10 cm in places. It has been determined that there are also vertical separations in some parts where these cracks occur (Fig. 9). These mass movements and vertical separations occurred as a result of the triggering of main shocks and aftershocks depending on the lithology, slope and climatic conditions of the region.



**Fig. 9** Views of soil surface cracks on the highways by the earthquake (Çevrimtaş village, Sivrice)



**Fig. 10** Çevrimtaş village damages

These geotechnical findings were detected in places close to the Sivrice district, and such findings were not encountered in locations further away from the district center. Sivrice district center and its villages, where the greatest geotechnical damage occurred, are the locations where the damage occurred the most in general. The most important reason for this situation is that the Sivrice district center is located at a place where the Pütürge Segment reaches Hazar Lake (Fig. 2). The Pütürge Segment is traced as a fault bundle approximately 1.5 km wide in the vicinity of Sivrice. Although part of the district center is on the bedrock, part of it is built on the alluvial deposits and part of it is built on the coastal sediments of Lake Hazar. All these geological and tectonic effects are considered as the factors causing damage in the district center (MTA Report 2020).

## 4 Damage Assessment of Masonry Buildings

Masonry buildings are the most preferred construction method for housing and other needs in rural areas of Türkiye. However, these buildings were generally built with poor workmanship and construction quality. This situation makes the buildings vulnerable to earthquake effects and causes damage in the earthquake. In this section, the structural damages observed in masonry buildings and their causes are detailed in the field surveys carried out in rural areas of Elazığ after the January 24, 2020 Sivrice-Elazığ earthquake.

### 4.1 Poor Workmanship and Binder Damages

During field observation, it was noted that almost all stone masonry buildings were constructed with weak mud mortar binders. It was observed that most of the buildings in the area were heavily damaged and some of them were destroyed (Fig. 10).

Buildings in rural areas are generally built without engineering service. Therefore, the workmanship and construction quality of the structures is generally poor. This situation caused the buildings to be weak against the effects of earthquakes and to receive heavy damage. Lime mortar supported with cement or cement mortar should be used as binder mortar in load-bearing walls depending on earlier TEC (1998) and TEC (2007). Furthermore, according to TBEC (2018), the minimum compressive strength of mortar for unreinforced masonry should be at least 5.0 MPa.

### 4.2 Out of Plane Mechanism

In masonry buildings, wooden beams that carry the weight of the floors are placed on the load-bearing walls in one direction only. The dynamic loads that occur during the earthquake are transferred to the perpendicular walls by these wooden beams. If a masonry structure has not vertical and horizontal bond beams that ensure the integrity of the structure, masonry walls not supported by wooden beams can be overturned in out-of-plane direction. Masonry buildings damaged due to out-of-plane mechanism in the affected region of the earthquake are shown in Fig. 11.

In addition, Fig. 12 shows the damage caused by the absence of horizontal and vertical beams and the irregular use of different materials.

In order to prevent these damages in masonry buildings, the unsupported length of a wall should be limited by using perpendicular walls and vertical bond beams. Regulation rules for this situation are quite clear. In the TBEC (2018), some rules are given for the maximum unsupported lengths of load-bearing walls and distances between vertical bond beams in unreinforced and confined masonry buildings (Fig. 13).



Fig. 11 View of out-of-plane failure on load-bearing walls

### 4.3 In-Plane Mechanism

It is generally accepted that load-bearing masonry walls act like shear walls in resisting the horizontal forces caused by earthquakes. Shear forces increase with earthquake loading and in case of insufficient strength on the walls, shear cracks form and the structure is damaged. These cracks in load-bearing wall cracks can be triggered by several factors: (i) poor construction detailing and poor material properties; (ii) large window or door openings; (iii) excessive wall lengths without any side support; and (iv) insufficient interlocking between wall units. Figure 14 shows the damage due to shear cracking on the load-bearing walls of masonry buildings.

In-plane mechanism damages usually occur due to the absence of tie beams that add lateral strength to the walls. Therefore, masonry walls should be constructed with sufficient and suitable vertical and horizontal beams to increase lateral seismic performance. In this regard, TBEC (2018) rules are quite clear as mentioned above.

### 4.4 Damages Due to Absence of Lintels or Insufficient Lintel Length

Severe cracks were also observed at the window and door corners of the masonry buildings in the field area. The main causes of these damages are the absence of lintels or insufficient lintel length (Fig. 15).



**Fig. 12** Lack of horizontal and vertical bond beams and irregular use of different materials together

In order to prevent such damages, TBEC (2018) has specified the necessary rules about the dimensions of the door and window openings and the lintel lengths. Reinforced concrete lintels will be built above the door and window spaces. The length of the parts of the lintels that rest on the wall shall not be less than 200 mm. The lintel height shall not be less than 150 mm. The rules given in Fig. 16 shall be complied with in the door and window spaces to be left on the load-bearing walls.

#### 4.5 Weak Load-Bearing Walls Damages

Another damage seen in the fieldwork after the earthquake is cracks in masonry walls with weak load-bearing capacity

**Fig. 13** Limits of unsupported wall length for load-bearing wall (TBEC 2018)

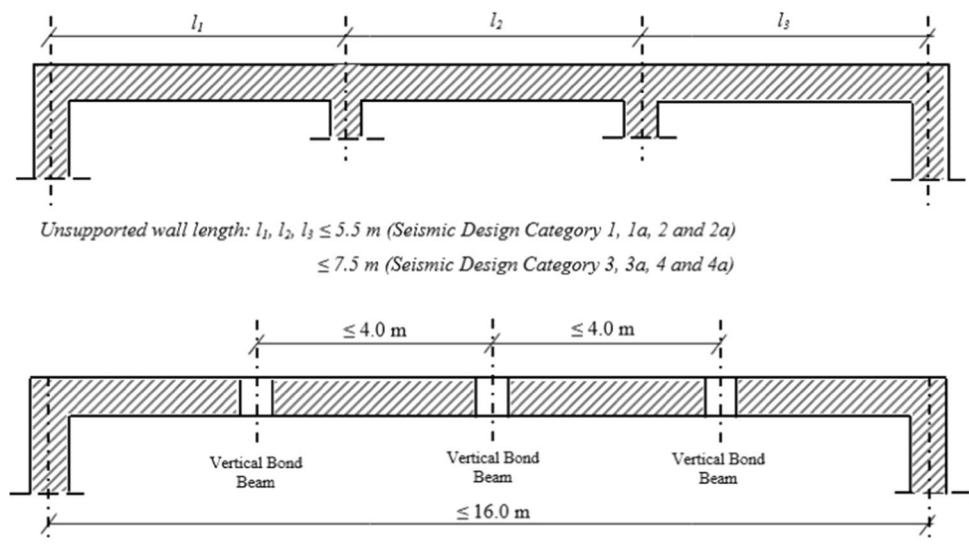


(Fig. 17). Earthquake Regulations have introduced some standards to prevent such damages and for masonry buildings to have a certain foundation capacity against vertical and horizontal forces.

In this line, TEC (1998) and (2007) stated that masonry walls can only be used in basements and ground floors, and the minimum thickness of load-bearing walls is limited to 0.50 m. The storey height is limited to 2.70 m and 3.0 m from the top of each floor to the next in adobe and stone masonry buildings. In addition, according to the current regulation, TBEC (2018), some rules have been introduced for masonry walls under the shear force (Table 3).

#### 4.6 Corner Damages

One of the major damages seen in existing masonry buildings in earthquake-affected areas is corner failure. This damage type results from poor wall-to-wall connections when forced by the out-of-plane mechanism. In case of an earthquake, vertical cracks develop, and wall corners are separated. Serious damages are caused because of weak connections among adjacent walls and the absence of bond beams. The corner damages at different buildings are shown in Fig. 18.

It is understood that the connections of the perpendicular walls of the masonry buildings are very important when looking at the damage in the pictures. Therefore, in masonry buildings, attention should be paid to the wall connections and should be designed in such a way that the system behaves as a whole.

#### 4.7 Multi-leaf Walls Damages

Multi-leaf walls are masonry elements, found frequently in many older and cultural heritage structures and our country masonry buildings. These walls are composed of successive

**Fig. 14** In-plane mechanism damages



masonry leaves connected with a considerably weaker, filler material, usually made of rubble and mortar and have a high percentage of voids. However, connections of these multi-leaf walls are weak generally. This weak joint results in the two leaves working almost independently, which may bring about their separation and therefore subsequent failure Valluzzi et al. (2001) under combined lateral and axial loading (Fig. 19). During the field survey, masonry structures damaged as a result of this weak connection were encountered (Fig. 20).

It was observed that the masonry buildings built in rural areas were damaged due to the above-mentioned reason under the influence of the earthquake.

## 5 Retrofitting Recommendations

Considering these types of damage caused by earthquakes, the earthquake performance of masonry buildings in earthquake-affected and high-seismic regions should be

reviewed. Structures with low seismic performance should be strengthened in order to prevent possible damage. In this section, some retrofitting methods suggested by some researchers are given to prevent such damage in existing masonry buildings. The retrofitting methods presented will contribute to the prevention of the above-mentioned types of damage.

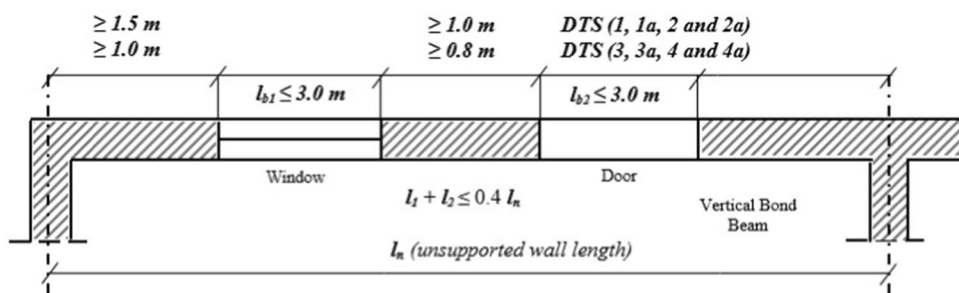
### 5.1 Strengthening of Masonry Walls with Reinforced Cement Coating

In this retrofitting case (Fig. 21), one places thin (less than 10 cm) layers of coating of cement reinforced with steel on masonry walls. The coating increases the wall's strength and ductility. It can be placed on the outside or the inside or both, depending on the most accessible areas. To enable the behavior of both elements (existing and new) to work together one places steel connectors on the wall.

**Fig. 15** Examples of cracks at corners of windows and doors of masonry buildings in Sivrice district



**Fig. 16** Specified requirements for window and door openings (TBEC 2018)



### 5.2 Strengthening of Masonry Walls with Polypropylene Meshing

Polypropylene (PP) mesh used in reinforced masonry buildings has been applied in Nepal, Pakistan and recently in China. PP retrofitting is used to encase masonry walls (Fig. 22), preventing both collapse and the escape of debris during earthquakes. This method is low-cost and easiest to implement in reinforcing conventional masonry buildings.

### 5.3 Strengthening with Composite Materials (CFRP and GFRP)

Another method used in the reinforcement of masonry buildings is the reinforcement of walls with composite materials, such as carbon fiber-reinforced polymer (CFRP) and glass fiber-reinforced polymer (GFRP). Figure 23 shows the application of CFRP/GFRP on a building wall. In this method, there can be placed also connectors, especially on walls, so that the material is well bonded to the masonry.



**Fig. 17** Vertical cracks in low-strength masonry

**Table 3** Geometric conditions to be applied in masonry walls under the effect of shear force (TBEC 2018)

Masonry type	$(t_{ef})_{min}$ (mm)	$(h_{ef} / t_{ef})_{max}$
Unreinforced masonry, with natural or artificial cut stone	350	9
Unreinforced masonry with other masonry units	240	12
Besieged masonry building	240	15
Reinforced masonry building	240	15
Reinforced panel systems	200	15

$t_{ef}$  The effective thickness of the wall

$h_{ef}$  The effective height of the wall



**Fig. 18** Examples of corner damages

#### 5.4 Strengthening Reinforced Concrete Shear Wall

In this method, the masonry wall is reinforced with a reinforced concrete shear wall (Fig. 24a). For the system to behave together, the shear wall and the masonry wall are connected with a sufficient number of anchors (Fig. 24b). Thus, the overall rigidity of the system can increase the lateral strength and control the slips between floors.

#### 5.5 Transversal Anchorage System

The middle layer between multi-layer walls as shown in Fig. 25 is typically composed of rubble stones of low quality and binding material that primarily serve as fillers. Transversal anchorage systems prevent the separation of two layers during an earthquake and significantly increase the strength of the structure by providing a connection between the two surfaces.

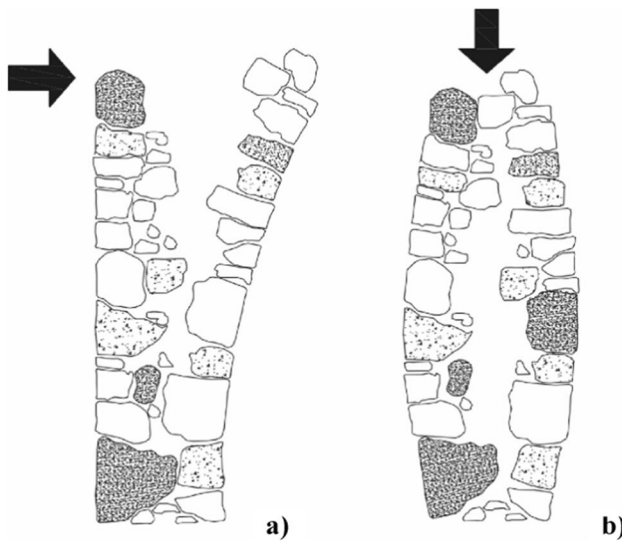


**Fig. 19** **a** Failure mechanism of a double-leaf wall panel subjected to a horizontal load. **b** Failure mechanism of a panel subjected to a compression vertical load (Corradi et al. 2017)

### 5.6 Improving the Connection Floor/Wall

Under earthquake effects, adding a horizontal buttress made of diagonally arranged steel ties to the wooden floor will make a positive contribution. With L-shaped steel plates, the connection between the ground and the masonry wall will be strengthened, so that the entire wall will meet the earthquake load, not pointwise (Fig. 26).

## 6 Conclusions and Recommendations

On January 24, 2020 an earthquake with a magnitude ( $M_w$ ) of 6.8 struck the Elazığ province, Türkiye. The earthquake caused the loss of 41 lives including 37 people in Elazığ and 4 people in Malatya and injured more than 1600 people. In the rural areas surrounding Elazığ, many masonry buildings were severely damaged or demolished. The purpose of this paper is to summarize the tectonic characteristics of the EAFZ, the seismic characteristics of the earthquake territory, the general characteristics of the main shock. In addition, another aim of this article is to reveal the damages caused by the earthquake in the masonry buildings in the rural area of Elazığ, by the post-earthquake field observations.

In addition, some application methods for strengthening existing masonry buildings with low seismic performance against future earthquakes are presented.

The following conclusions can be drawn from the field investigations:

- In the rural areas of Elazığ province, most of the buildings were constructed of masonry. It was found that these buildings were generally constructed with local materials, often without engineering services and using traditional techniques, as one or two-story buildings, with or without basements.
- The main causes of damage or collapse of masonry buildings were poor quality of workmanship and construction, the inadequate material characteristics of the masonry walls, weak load-bearing walls (lack of horizontal or vertical bond beams, large unsupported wall lengths, absence or inadequate lintel length, etc.).
- The out-of-plane and in-plane mechanism is one of the main structural damages in masonry buildings. The main defects causing this damage are the absence of vertical and horizontal bond beams, weak connections between walls, and large unsupported walls. In addition, many masonry buildings failed to reflect the diaphragm action, resulting in partial damage or collapse of the buildings.
- Corner damage was observed due to weak wall-to-wall connections and the absence of vertical and horizontal beams. The use of sufficient beams, in accordance with the seismic code, and the use of appropriate wall-to-wall or wall-to-wall adhesive connections can eliminate such damage.
- The masonry buildings in the rural surroundings of Elazığ were not designed and constructed in accordance with the requirements of the contemporary Türkiye Earthquake Codes.

Finally, the January 24, 2020 Sivrice-Elazığ earthquake shows that masonry buildings constructed in rural areas of Elazığ are highly vulnerable to future earthquakes. In order to improve the performance of existing masonry buildings in future earthquakes, the building stock should be examined and those with low performance should be strengthened with the methods suggested in the study or with other techniques. In addition, new masonry buildings should be constructed according to contemporary design codes.





Fig. 20 Walls poorly constructed stone masonry building

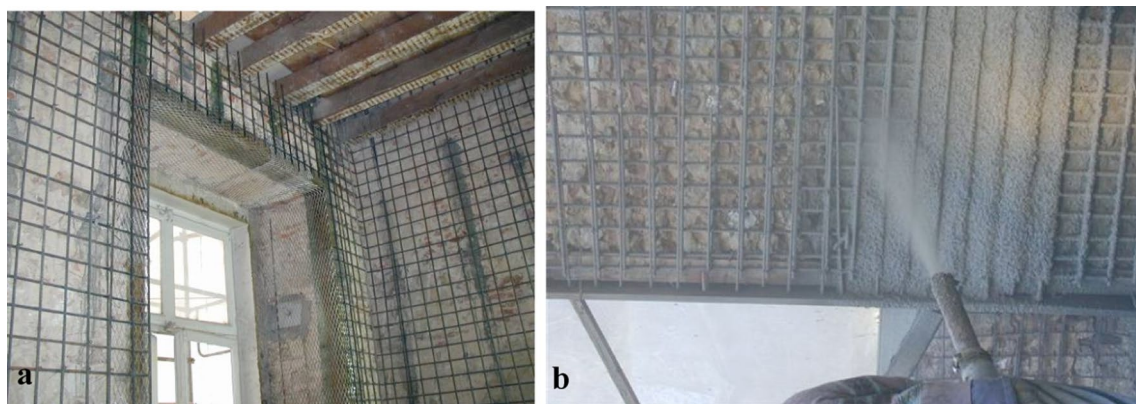
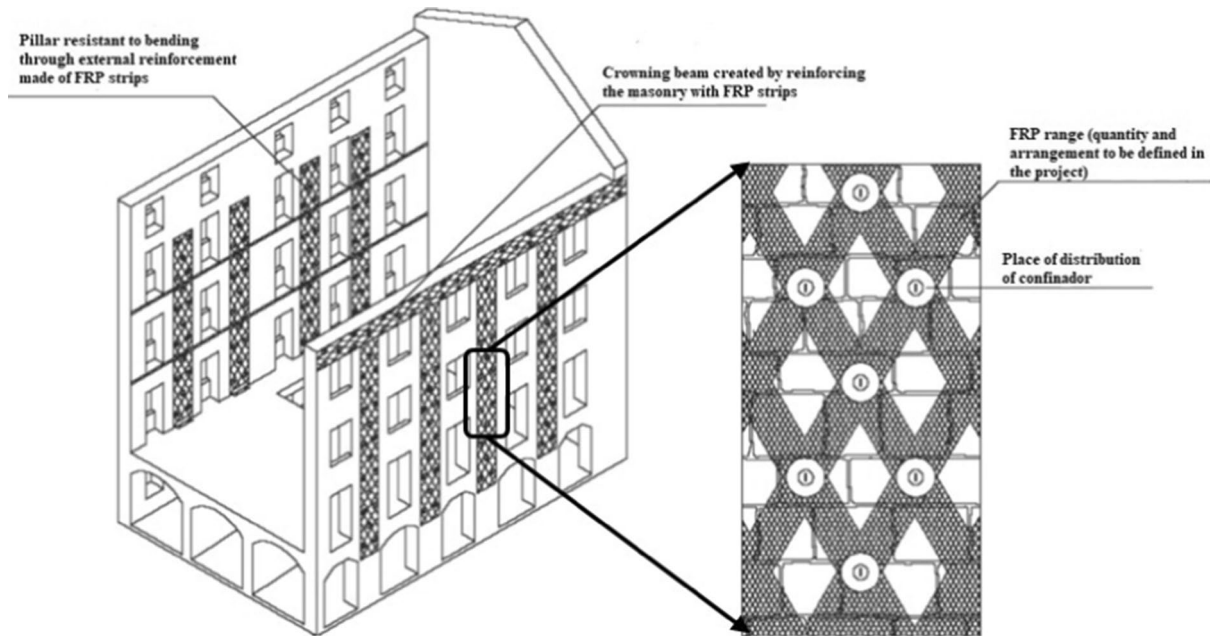


Fig. 21 a Masonry wall from the inside with steel mesh, b spraying of the cement grout into the wall (Adopted from Appleton 2009)

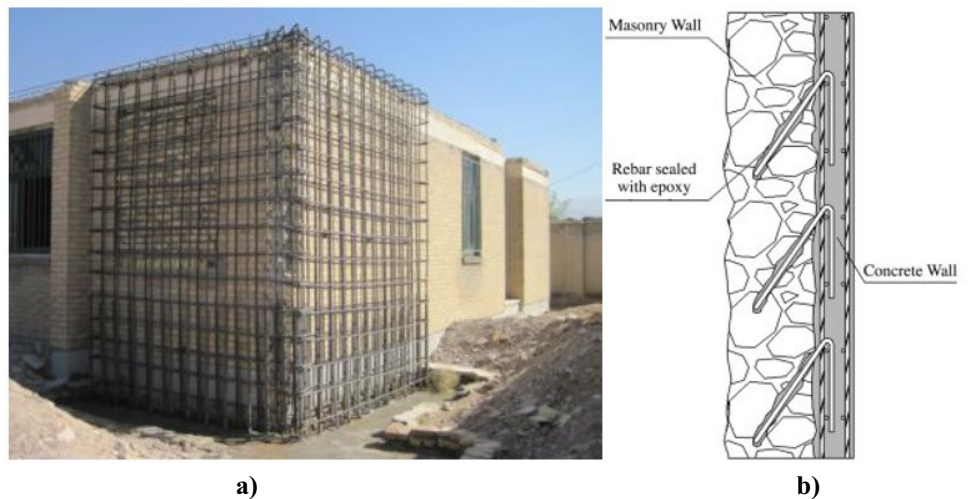


**Fig. 22** Implementation of the PP band method of retrofitting in Kathmandu Valley (left) and anchorage throughout the wall (right) (Adopted from Shrestha et al. 2012)



**Fig. 23** Application of CFRP/GFRP on a building wall (Adopted from Henriques et al. 2011)

**Fig. 24 a** Application of RC concrete shear wall (Adopted from Mahdizadeh et al. 2012) **b** sectional view (Adopted from Branco and Guerreiro 2011)



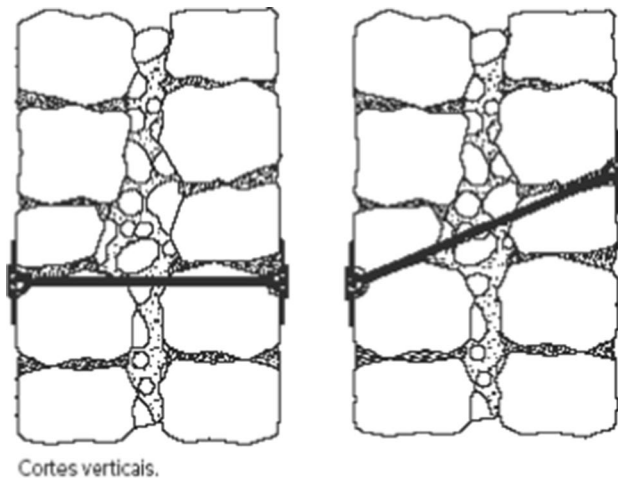


**Fig. 25** Transversal anchorage system in multi-layer masonry walls (Adopted from Meireles and Bento 2013)



**Fig. 26** Transversal anchorage system in multi-layer masonry walls (Adopted from Meireles and Bento 2013)

**Acknowledgements** This work was supported by the Scientific Research Projects Coordination Unit of Fırat University (Grant Numbers ADEP.23.13).

**Funding** This work was supported by Scientific Research Projects Coordination Unit of Fırat University (Grant Numbers ADEP.23.13).

## Declarations

**Conflict of interest** The authors declare the following financial interests/personal relationships, which may be considered as potential competing interests: This work was supported by Scientific Research Projects Coordination Unit of Fırat University (Grant Numbers ADEP.23.13).

**Ethical Approval** The manuscript was not be submitted to more than one journal for simultaneous consideration. The submitted work is original and has not been published elsewhere in any form or language (partially or in full). A single study was not be split up into several parts to increase the quantity of submissions and submitted to various jour-

nals or to one journal over time. Results are presented openly, honestly, and without fabrication, falsification, or inappropriate data manipulation (including image-based manipulation). No data, text or theory of others is presented as the authors' own. Appropriate acknowledgments were given to other studies.

## References

- Appleton J (2009) Técnicas de reabilitação de estruturas de alvenaria, Seminar Patologia, Inspeção e Reabilitação de Edifícios tradicionais (in Portuguese)
- Basaglia A, Aprile A, Spacone E, Pelà F (2020) Assessing community resilience, housing recovery and impact of mitigation strategies at the urban scale: a case study after the 2012 Northern Italy Earthquake. *Bull Earthq Eng* 18:6039–6074
- Bayraktar A, Altunışık AC, Pehlivan M (2013) Performance and damages of reinforced concrete buildings during the October 23 and November 9, 2011 Van, Turkey, earthquakes. *Soil Dynam Earthq Eng* 53:49–72
- Bayraktar A, Altunışık AC, Muvafik M (2014) Damages of minarets during Erciş and Edremit earthquakes, 2011 in Turkey. *Smart Struct Syst* 14(3):479–499
- Bayraktar A, Altunışık AC, Türker T, Karadeniz H, Erdoğan Ş, Angın Z, Özşahin TŞ (2015) Structural performance evaluation of 90 RC buildings collapsed during October 23 and November 9, 2011 Van, Turkey, earthquakes. *J Perform Constr Facilit ASCE* 29(6):1–19
- Bozkurt E (2001) Neotectonics of Turkey—A synthesis. *Geod Acta* 14:3–30
- Branco M, Guerreiro LM (2011) Seismic rehabilitation of historical masonry buildings. *Eng Str* 33:1626–1634
- Brando G, De Matteis G, Spacone E (2017) Predictive model for the seismic vulnerability assessment of small historic centres: application to the inner Abruzzi Region in Italy. *Eng Struct* 153:81–96
- Calayır Y, Sayın E, Yön B (2012) Performance of structures in the rural area during the March 8, 2010 Elazığ-Kovancılar earthquake. *Nat Haz* 61(2):703–717
- Celep Z, Erken A, Taskin B, Ilki A (2011) Failures of masonry and concrete buildings during the March 8, 2010 Kovancılar and Palu (Elazığ) Earthquakes in Turkey. *Eng Fail Anal* 18:868–889
- Corradi M, Borri A, Poverello E, Castori G (2017) The use of transverse connectors as reinforcement of multi-leaf walls. *Mater Struct* 50:114
- Dedeoğlu İÖ, Yetkin M, Calayır Y (2022) 24 January 2020 Sivrice-Elazığ earthquake: assessment of seismic characteristics of earthquake, earthquake territory and structural performance of reinforced concrete structures. *Sakarya Univ J Sci* 26(5):1892–1907. <https://doi.org/10.16984/saufenbilder.1005024>
- DEMA (2020a) January 24, 2020 Sivrice (Elazığ) earthquake report. Earth Dep Dis A Emerg Manag Pres, Ankara, Turkey
- DEMA (2020b) Earthquake department of the disaster and emergency management presidency. Ankara, Turkey. <http://www.afad.gov.tr/>
- Doğangün A (2004) Performance of reinforced concrete buildings during the May 1, 2003 Bingöl earthquake in Turkey. *Eng Str* 26:841–856
- Günaydın M, Atmaca B, Demir S, Altunışık AC, Hüsem M, Adanur S, Ateş Ş, Angın Z (2021) Seismic damage assessment of masonry buildings in Elazığ and Malatya following the 2020 Elazığ-Sivrice earthquake, Turkey. *Bull Earth Eng* 19:2421–2456
- Henriques DF, Nunes L, de Brito J (2011) Reabilitação Estrutural de Edifícios Antigos—Alvenaria, Madeira—Técnicas pouco intrusivas. Ed. Argumentum & Gecorpa. In CIMAD 11—1º Congresso

- Ibero-Latino Americano da madeira na construção 279–280, Lisbon, Portugal (in Portuguese)
- Hosseini M (2005) Behavior of nonstructural elements in the 2003 Bam, Iran, earthquake. *Earthq Spect* 21:439–453
- Kürçer A, Elmacı H, Yıldırım N, Özalp S (2020) January 24, 2020 Sivrice (Elazığ) Depremi (Mw = 6.8) Field observation and evaluation report. *Min Res A Expl Inst*, Ankara (in Turkish)
- Mahdizadeh A, Borzouie J, Raessi M, (2012) New approach to seismic rehabilitation of masonry school buildings. *Proc. 15th W Conf Earth Eng*, Lisbon, Portugal 2851, Lisbon, Portugal
- Marroni M, Göncüoğlu MC, Frassi C, Sayit K, Pandolf L, Ellero A, Ottria G (2020) The Intra-Pontide ophiolites in Northern Turkey revisited: from birth to death of a Neotethyan oceanic domain. *Geosci Front* 11(1):129–149
- Meireles H Bento R (2013) Rehabilitation and strengthening of old masonry buildings. Report ICIST, DTC, (02)
- MTA-Mineral Research and Exploration General Directorate (2020) January 24, 2020 Sivrice (Elazığ) Earthquake Report
- Okay AI, Zattin M, Cavazza W (2010) Apatite fission-track data for the Miocene Arabia-Eurasia collision. *Geology* 38(1):35–38
- Ricci P, Luca F, Verderame GM (2011) 6th April 2009 L'Aquila earthquake, Italy: reinforced concrete building performance. *Bull Earth Eng* 9:285–305
- Rossetto T, Peiris N (2009) Observations of damage due to the Kashmir earthquake of October 8, 2005 and study of current seismic provisions for buildings in Pakistan. *Bull Earth Eng* 7:681–699
- Şaroğlu F, Emre Ö, Kuşcu İ (1992) The East Anatolian fault zone of Turkey. *Ann Tect* 6:99–125
- Sayin E, Yon B, Calayir Y, Gor M (2014) Construction failures of masonry and adobe buildings during the 2011 Van earthquakes in Turkey. *Struct Eng Mech* 51(3):503–518
- Sayin E, Yon B, Onat O, Gör M, Öncü ME, Tuğ ET, Bakır D, Karaton M, Calayir Y (2021) 24 January 2020 Sivrice-Elazığ, Turkey earthquake: geotechnical evaluation and performance of structures. *Bull Earth Eng* 19:657–684
- Sezen H, Whittaker AS, Elwood KJ, Mosalam KM (2003) Performance of reinforced concrete buildings during the August 17, 1999 Kocaeli, Turkey earthquake, and seismic design and construction practise in Turkey. *Eng Str* 25:103–114
- Sharma K, Deng L, Noguez CC (2016) Field investigation on the performance of building structures during the April 25, 2015, Gorkha earthquake in Nepal. *Eng Struct* 121:61–74
- Shrestha H, Pradhan S, Guragain R (2012) Experiences on retrofitting of low strength masonry buildings by different retrofitting techniques in Nepal. *Proc. 15th W Conf Earth Eng*, Lisbon, Portugal
- Sisti R, Di Ludovico M, Borri A, Prota A (2019) Damage assessment and the effectiveness of prevention: the response of ordinary unreinforced masonry buildings in Norcia during the Central Italy 2016–2017 seismic sequence. *Bull Earthq Eng* 17:5609–5629
- TBEC (2018) Disaster and emergency management presidency, Türkiye Bina Deprem Yönetmeliği (in Turkish)
- TEC (1998) Ministry of public works and housing, Afet Bölgelerinde Yapılacak Yapılar Hakkında Yönetmelik (in Turkish)
- TEC (2007) Ministry of public works and housing, Deprem Bölgelerinde Yapılacak Binalar Hakkında Esaslar, Disaster and Emergency Management Presidency, (in Turkish)
- Valluzzi MR, da Porto F, Modena C (2001) Behaviour of multi-leaf stone masonry walls strengthened by different intervention techniques. *Hist Const* 1023–1032
- Yetkin M, Dedeoğlu İÖ, Calayir Y (2021) Investigation and assessment of damages in the minarets existing at Elazig after 24 January 2020 Sivrice earthquake. *Firat Univ J Eng Sci* 33(2):379–389

Springer Nature or its licensor (e.g. a society or other partner) holds exclusive rights to this article under a publishing agreement with the author(s) or other rightsholder(s); author self-archiving of the accepted manuscript version of this article is solely governed by the terms of such publishing agreement and applicable law.